EVALUATION OF HCFeMn AND SiMn SLAG TAPHOLE PERFORMANCE USING CFD AND THERMOCHEMICAL PROPERTY MODELLING FOR CaO-MnO-SiO_2-Al_2O_3-MgO SLAG

J. Muller, J.D. Steenkamp

Dept. of Materials Science and Metallurgical Engineering, University of Pretoria, Pretoria, South Africa

ABSTRACT

The tapping of slag and metal is a key operational aspect in high-carbon ferromanganese (HCFeMn) and silicomanganese (SiMn) production, which is influenced mostly by the taphole design and thermochemical properties. Unfavourable behaviour includes difficulties during taphole opening, and sluggish or intermittent slag flow. The slags consist mostly of components in the CaO-MnO-SiO_2-Al_2O_3-MgO system, but differ greatly in MnO content and basicity, due to the different process routes followed and thermodynamic requirements.

To accurately model the flow behaviour, the latest thermochemical property models were applied. Viscosity, thermal conductivity, density, and heat capacity were modelled as functions of temperature for typical HCFeMn and SiMn slag compositions. These were used in slag tapping simulations set up in computational fluid dynamics (CFD) modelling software and executed to gain insight into heat and mass flow behaviour, and how slag tapping could be optimized in terms of slag chemistry, taphole design, and possibly other operational practices.

This paper presents the combined effects of the differences in thermochemical properties of typical HCFeMn and SiMn slags as results of the CFD modeling. With the focus on the effects of chemical and thermal differences, the modelled domain was simplified by considering a simple slag bath. The heat and mass transfer behaviour is simulated during a tap and from tap-to-tap, considering typical time periods for each.

KEYWORDS: *Slag, CFD, taphole, high-carbon ferromanganese, silicomanganese, thermochemical properties.*

1. INTRODUCTION

The manganese-bearing slag of interest is a by-product in the production of manganese ferroalloys, which are classified into ferromanganese (FeMn), and silicomanganese (SiMn) [1]. Submerged-arc furnaces (SAFs) are predominantly used to produce these by smelting manganese oxide ores and reductants. In South African practices, high-carbon ferromanganese (HCFeMn) slags contain 15% to 20% MnO, and SiMn slags approximately 9% MnO, and are in both cases discarded onto slag dumps. In other countries, HCFeMn slags contain typically 30% to 50% MnO (high-MnO slag practice), and are used as feedstock to produce SiMn [2]. SiMn process temperatures range from 1600°C to 1650°C with the slag leaving the furnace between 1550°C and 1650°C, while process temperatures in HCFeMn production range between 1400°C and 1500°C [2].

Typical lining and taphole refractory configurations exist for the production of manganese ferroalloys. A typical taphole configuration is the insulating type, where ceramic refractories are utilized with low thermal conductivity that limits heat losses [3]. Conductive carbon-based refractories adopted in recent times, with high thermal conductivities, result in a high heat flux that promotes the formation of protective freeze linings [4]. Slag tapping occurs typically every 2 hours, lasting around 20 to 40 minutes [5]. From typical production figures for HCFeMn and SiMn furnaces [2], it is calculated that between 16 and 21 t of slag is tapped every 2 hours, relating to taphole velocities of 0.5 to 0.7 $m.s^{-1}$ (assuming a 20 minute tap duration and taphole diameter of 100 mm).

Operational difficulties experienced during tapping include slag taphole opening and sluggish or intermittent slag flow during tapping, which can be related to differences in operating conditions and chemical composition (thermochemical properties). These are compensated for by typically increasing the operating temperature, changing the slag chemistry, or lancing open tapholes. This causes increased refractory damage over time, as well as other adverse effects on the process and equipment. The CaO-MnO-SiO_2-Al_2O_3-MgO slag system is therefore studied to understand the underlying differences in the production of HCFeMn and SiMn specifically related to the influences of slag composition. Typical slag compositions, partly sourced from literature [2], have been identified for evaluation, consisting mostly of components from the CaO-MnO-SiO_2-Al_2O_3-MgO slag system (table 1).

Table 1: Typical HCFeMn and SiMn slags

Name	Reference	Normalized composition, mass%					Basicity*
		MnO	SiO_2	Al_2O_3	CaO	MgO	
HCFeMn Slag A	High MnO slag[2]	40.9	23.1	12.7	16.9	6.4	1.79
HCFeMn Slag B	Discard slag[2]	15.1	24	20.7	34.4	5.7	1.23
HCFeMn Slag C		29.8	30	4.3	29.3	6.6	1.91
HCFeMn Slag D		36	24	16	20	4	1.5
SiMn Slag A	Typical SiMn slag[2]	8.5	45.2	15.8	21	9.5	0.64
SiMn Slag B		7.7	42.1	20.9	22.4	6.9	0.59
SiMn Slag C		3.1	41.8	20	29	6.2	0.62

*Basicity = (CaO+MgO+MnO)/(Al_2O_3+SiO_2)

2. METHODOLOGY

The flow of manganese-bearing slag through an electric furnace taphole with an insulating lining is modelled using computational fluid dynamics (CFD) modelling software ANSYS FLUENT [6]. Heat transfer and mass flow are modelled according to the conservation of energy and momentum, which require the thermochemical property values of slag and refractories (thermal conductivity, heat capacity, density and viscosity) [7]. To accurately model the flow behaviour, the latest thermochemical property models were applied using also the computational thermochemistry software FactSage [8]. The typical HCFeMn and SiMn slags (table 1) were evaluated as functions of temperature and chemicals composition, with the models and results published elsewhere [9]. With the developed models the heat and mass transfer behaviour is simulated and evaluated during a tap and from tap-to-tap, considering typical time periods for each. Steady-state and transient model scenarios were defined for evaluation, varying the slag properties, material specifications in some areas (slag liquid or taphole clay), and boundary conditions (process temperature). This included baseline models simulating steady states with the taphole closed, used as initial conditions to the transient tapping simulations of 20 minutes with the taphole open. The final states of the tapping simulations were used as initial conditions to the transient simulation of 100 minutes with the taphole closed with taphole clay.

3. CFD MODEL CONFIGURATION

CFD modelling software ANSYS FLUENT was used to model heat and mass transfer through the taphole of a SAF with a ceramic-based insulating lining in two dimensions. The domain representing the refractory layout was drawn, a mesh generated, and the heat and mass flow models set up with boundary conditions and other required configurations to execute different steady-state and transient scenarios. In ANSYS FLUENT, the k-ε turbulence model was used to model mass flow [6].

3.1. Domain

The chosen domain represents a typical as-built insulating refractory lining and taphole configuration (figure 1), composed of layered alumina silicate and silicon carbide refractories. A taphole diameter of 100 mm is specified, plugged with taphole clay after tapping. It includes a simplified slag bath on the hot-face of the taphole, and a carbon paste hearth top layer. These simplifications are assumed to remain unchanged with the focus on the comparative evaluation of the slags. The steel shell has also been excluded from the domain, simplifying the model mesh without significantly influencing the modelled heat transfer.

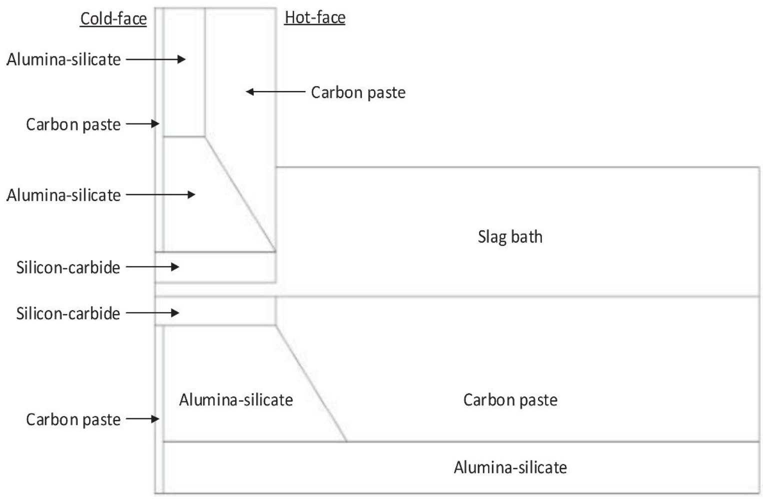

Figure 1: Insulating lining domain configuration applied in the CFD model

3.2. Boundary conditions

The following boundary conditions have been defined around the model domain (figure 1):

- **Furnace inside symmetry plane**: Only one half of the cylindrical furnace lining is considered, with the inside of the domain defined as a symmetry plane.
- **Furnace floor and lower sidewalls cold-face**: Forced convection boundary condition with a heat transfer coefficient of 30 $W.m^{-2}.K^{-1}$ calculated using a free stream temperature of 25°C and other relevant conditions [10].
- **Tapblock cold-face**: Natural convection boundary with a heat transfer coefficient of 5 $W.m^{-2}.K^{-1}$ calculated using a free stream temperature of 25°C and other relevant conditions [10].
- **Taphole outlet**: Pressure outlet for slag flow during the tapping simulation [6], and a natural convection boundary condition when the taphole is closed (same as tapblock cold-face).
- **Upper sidewalls cold-face**: Thin-film water cooling with a constant of 55°C assumed.
- **Top of upper sidewalls**: Heat transfer predominantly in the horizontal (radial) direction, with an insulated boundary condition assumed and no heat flux perpendicular to the face.
- **Hot-face upper sidewalls:** Constant temperature (HCFeMn: 1400°C, SiMn: 1600°C).
- **Slag bath top**: Zero pressure inlet and constant temperature boundary conditions [6]. Temperature is the same as the hot-face of the upper sidewall boundary.

3.3. Material Properties

Solid refractory material properties were sourced from datasheets from manufacturers of typical examples of the materials used [11,12] and other literature sources [13], summarized in table 2. Values are assumed for taphole clay, with minimal impact on the model results accuracy.

For each of the HCFeMn and SiMn slag compositions considered for evaluation (table 1), property values of viscosity, thermal conductivity, density, and heat capacity have been modelled as functions of temperature [9], summarized in table 3 for the typical operating temperatures of 1400°C for HCFeMn slags and 1600°C for SiMn slags.

Table 2: Summary of solid material physical properties

Type	Application	Thermal conductivity, $W.m^{-1}.K^{-1}$	Heap capacity, $J.kg^{-1}.K^{-1}$
Nitride-bonded silicon-carbide [11]	Ceramic refractories used in the tapblock	16.3 $W.m^{-1}.K^{-1}$ @ 1204°C	1169.2 $J.kg^{-1}.K^{-1}$
Alumina-silica [12]	Ceramic refractories used in the sidewalls	1.2 $W.m^{-1}.K^{-1}$ @ 1000°C	1311.3 $J.kg^{-1}.K^{-1}$
Carbon paste [13]	Carbon-based filler material used on the hot face of the upper sidewalls, as sacrificial layer on the floor, and as filler material on the cold face of the walls	3.2 $W.m^{-1}.K^{-1}$ @ 200°C 6.8 $W.m^{-1}.K^{-1}$ @ 500°C 19.2 $W.m^{-1}.K^{-1}$ @ 1000°C 30.3 $W.m^{-1}.K^{-1}$ @ 1400°C 37.1 $W.m^{-1}.K^{-1}$ @ 1800°C	1162 $J.kg^{-1}.K^{-1}$ @ 200°C 1619 $J.kg^{-1}.K^{-1}$ @ 500°C 1925 $J.kg^{-1}.K^{-1}$ @ 1000°C 2034 $J.kg^{-1}.K^{-1}$ @ 1400°C 2097 $J.kg^{-1}.K^{-1}$ @ 1800°C
Taphole clay	Material used to fill the taphole after tapping	10 $W.m^{-1}.K^{-1}$	1000 $J.kg^{-1}.K^{-1}$

Table 3: Thermochemical properties calculated for the typical slag compositions (table 1) of HCFeMn slags at 1400°C and SiMn slags at 1600°C

	Solidus temperature, °C	Liquidus temperature, °C	Density, $kg.m^{-3}$	Effective viscosity, Poise	Thermal conductivit, $W.m^{-1}.K^{-1}$	Heat capacity solid, $J.kg^{-1}.K^{-1}$	Heat capacity liquid, $J.kg^{-1}.K^{-1}$
HCFeMn Slag A	1122	1501	3327	15.4	0.182	963	1180
HCFeMn Slag B	1167	1419	3017	12.7	0.190	1083	1215
HCFeMn Slag C	1129	1444	3127	6.4	0.146	975	1173
HCFeMn Slag D	1106	1323	3317	14.4	0.165	970	1168
SiMn Slag A	1072	1233	2774	7.4	0.200	1110	1260
SiMn Slag B	1075	1310	2795	9.2	0.217	1141	1254
SiMn Slag C	1072	1296	2745	7.4	0.205	1197	1241

4. RESULTS AND DISCUSSION

The baseline steady-state models simulating the temperature profiles in the lining before tapping, with the taphole closed, varied only in slag thermochemical and hot-face temperature boundary conditions (1400°C for HCFeMn and 1600°C for SiMn slag). Temperature differences of less than 10°C were predicted per type of slag, indicating the effect of differences in chemical composition to be negligible under these conditions. On the hot-face (figure 2 a) refractory temperatures were found to be between 60°C and 141°C lower than the bulk HCFeMn slag (1400°C), and between 77°C and 189°C lower than the bulk SiMn slag (1600°C). Also with the taphole closed, temperatures on the hot-face were on average 157°C lower in the HCFeMn process compared to SiMn (figure 2 a), and 65°C on average lower on the cold-face (figure 2 b). Overall temperatures are lower in the bottom of the tapblock as affected by the conductive hearth top layer (figure 2 a). At this steady state, heat flux from the tapblock cold-face are predicted to vary between 2.8 and 3.2 $kW.m^{-2}$ (table 4), with the SiMn process heat flux higher due to the elevated operating temperature.

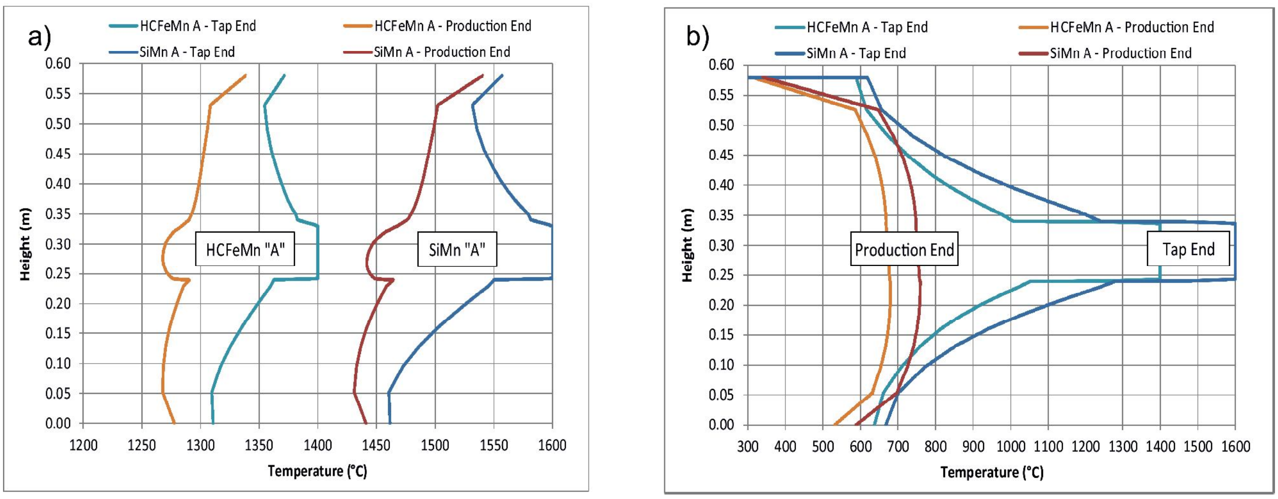

Figure 2: Temperatures on vertical profiles through the tapblock at steady state with the taphole open and closed operating with HCFeMn "A" and SiMn "B" at a) hot-face and b) cold-face surfaces of the tapblock

Table 4: Tap stream and tapblock parameter values at the end of simulations with the taphole open and closed, operating with different HCFeMn and SiMn slags

	Taphole Closed	**Taphole Open**			
Slag	**Tapblock heat flux, $kW.m^{-2}$**	**Av. velocity, $m.s^{-1}$**	**Av. wall shear, Pa**	**Tapblock heat flux, $kW.m^{-2}$**	**Tap stream heat transfer coeff. (constant area), $kW.m^{-2}.K^{-1}$**
HCFeMn A	2.79	2.603	561	3.66	174.7
HCFeMn B	2.76	2.606	490	3.83	189.5
HCFeMn C	2.76	2.965	410	3.81	230.3
HCFeMn D	2.80	2.537	532	3.62	172.5
SiMn A	3.16	2.802	391	4.17	255.2
SiMn B	3.16	2.717	423	4.12	241.3
SiMn C	3.17	2.794	390	4.18	255.6

Temperatures increase during tapping mostly in the tapblock refractories, with the rest of the lining unaffected (figure 3). The effects of variations in the slag thermochemical properties are observed as differences in the average slag velocity. SiMn slags and HCFeMn "C" slag have slightly higher average velocities predicted (table 4), correlated to the lower viscosities of these slags at typical operating temperatures (table 3). During tapping, temperatures close to the tap stream are estimated to increase by as much as 130°C on the hot-face and 568°C on the cold-face in the case of SiMn slags, and for HCFeMn slags 86°C on the hot-face and 414°C on the cold-face (figure 2 b). Due to the increased velocity of slag HCFeMn "C", tapblock temperatures increased by up to 153°C more than other HCFeMn slags. Considering the transient results (figure 4 a) tapblock temperatures close to the tap stream would mostly increase as heat is absorbed from the tap stream, then decrease as heat is conducted away, but not reach steady state within the 20 minute simulation. Refractory temperatures close to the taphole would increase only for the slags HCFeMn "B" and "D" with the highest viscosities and lowest total temperature changes (figure 4 a).

When tapping, heat flux from the tap stream to the refractory increases from the hot-face towards the cold-face as the temperature difference increases along the path that the refractory temperature decreases. An almost constant heat transfer coefficient along the length of the taphole is obtained (figure 5), excluding approximately the first 0.2 m taphole entry region where the flow profile develops. Average heat transfer coefficients calculated for HCFeMn and SiMn slags increase for higher velocities predicted (table 4).

Similarly, the average wall shear calculated between the tap stream and refractory during tapping correlates with the average velocities, with lower values predicted for the SiMn slags and HCFeMn "C" slag (table 4).

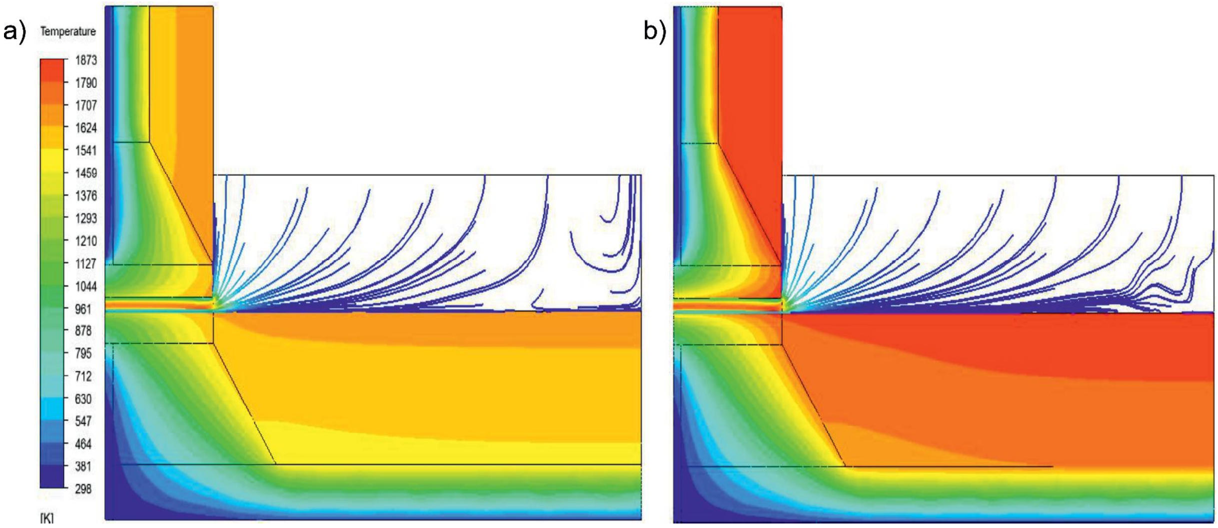

Figure 3: Temperature profiles and velocity stream lines at the end of the tapping simulation operating with a) HCFeMn "A" slag, and b) SiMn "A" slag

After the taphole is closed with taphole clay, refractory temperatures decrease quickly by up to 587°C (figure 4 a). Heat is absorbed from the refractories close to the taphole, but further away the refractories remain at the higher temperatures reached during tapping. Temperatures cycles are greatest close to the taphole center, and even more pronounced for the SiMn slags at higher tap stream temperatures. Temperature differences are also higher at the hot-face than at the cold-face.

During the rest of the 100 minutes after the taphole is closed, the temperatures in these regions around the taphole would then increase, while further away in the tapblock temperatures would decrease as the tap stream heat absorbed is conducted away.

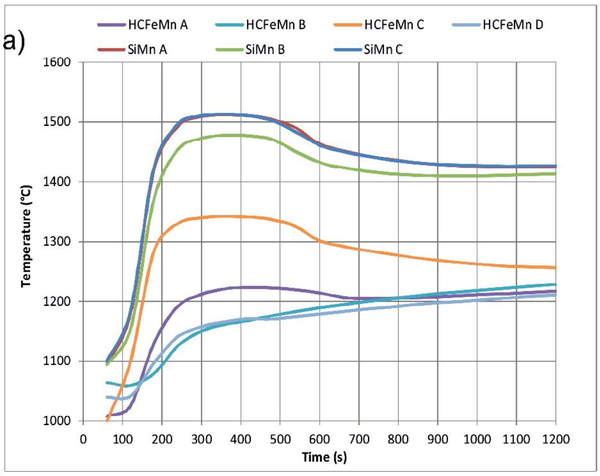

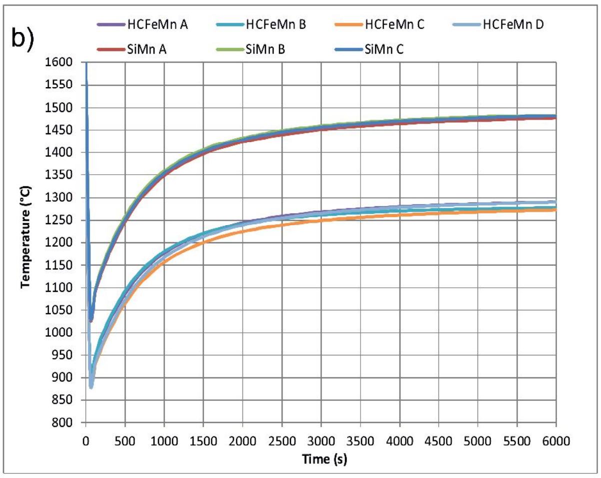

Figure 4: Temperatures versus time at the centre of the tapblock above the taphole operating with different HCFeMn and SiMn slags when a) the taphole is opened, and b) the taphole is closed

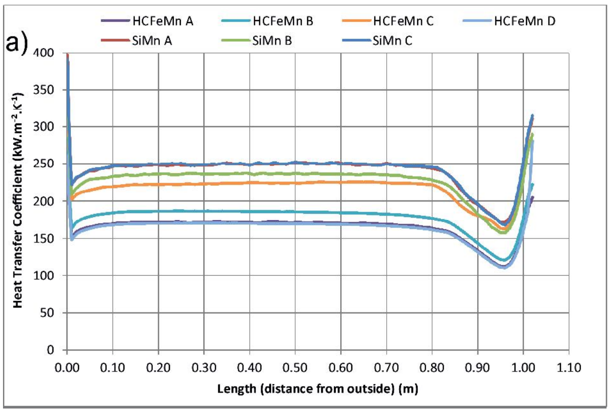

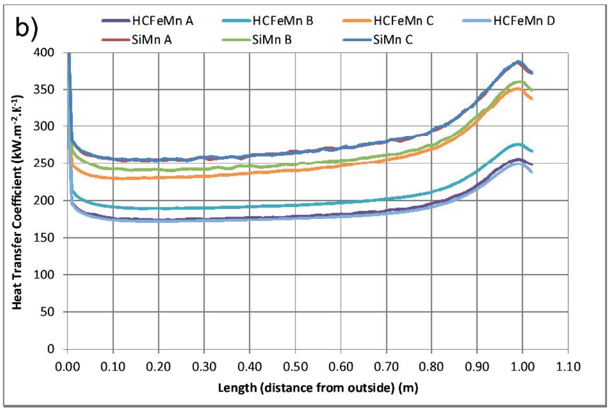

Figure 5: Heat transfer coefficients between the tap stream and the taphole refractory at the end of the tapping simulation operating with different HCFeMn and SiMn slags, at a) top of the tap stream, and b) bottom of the tap stream

5. CONCLUSION

In the production of HCFeMn and SiMn in SAFs the tapping of slag is an important operational aspect affected by operating temperatures, taphole refractory design and slag thermochemical properties that vary with chemical composition and temperature. For typical manganese-bearing slag compositions, notable differences are caused by significantly higher SiO_2 contents in SiMn slags in combination with the tapping temperature being 200°C higher than that for HCFeMn.

Steady-state baseline CFD simulations with the taphole closed showed small variations in tapblock temperatures at fixed points of less than 10°C due to slag chemical differences alone. Hot-face temperatures at this steady state are lower than the slag bath bulk by between 60°C and 189°C. During the 20 minute tapping, temperatures in the tapblock refractories are predicted to cycle by up to 568°C at the cold-face of the taphole. Average tapping velocities of 2.5 to 3.0 $m.s^{-1}$ are predicted, higher for the lower-viscosity SiMn and HCFeMn "C" slags. For these, higher heat transfer coefficients are predicted between the tap stream and taphole, resulting in tapblock temperature cycles of up to 153°C more than the HCFeMn slags with higher viscosities. After closing the taphole with clay, refractory temperatures decrease by up to 587°C close to the taphole. In the 100 minutes simulated with the taphole closed, these temperatures would then increase, while further away from the taphole the temperatures that increased during tapping would then decrease.

6. REFERENCES

[1] Habashi, F. Handbook of Extractive Metallurgy. Wiley-VCH, Weinheim, 1997, vol. 1, pp. 420–434.

[2] Olsen, S.E., Tangstad, M., and Lindstad, T. Production of Manganese Ferroalloys. SINTEF and Tapir Academic Press, Trondheim, 2007.

[3] Brun, H.Development of refractory linings for electric reduction furnaces producing Mn lloys at Elkem A/S, PEA Plant in Porsgrunn, Norway. J.Inst. Refract. Eng., Spring 1982, pp. 12.

[4] Hearn, M.H., Dzermejko, A.J., Lamont, P.H. “Freeze” lining concepts for improving submerged arc furnace lining life and performance. Proceedings: Eighth International Ferroalloys Congress INFACON 8: Transformation through Technology, Beijing, China, 7-10 June 1998, pp. 401-426.

[5] Mølnås, H.Compatibility study of carbon-based refractory utilised in silicomanganese production furnaces. NTNU, Trondheim, 2011.

[6] ANSYS®Academic Research, Release 13.0, Help System. ANSYS Inc., Canonsburg PA, USA.

[7] Versteeg, H.K. and Malalasekera, W. An Introduction to Computational Fluid Dynamics – The Finite Volume Method, 2nd edn. Prentice Hall, Englewood Cliffs, New Jersey, 2007.

[8] Bale, C.W., Chartrand, P., Degterov, S.A., Eriksson, G., Hack, K., Ben Mahfoud, R., Melançon, J., Pelton, A.D., and Petersen, S. FactSage thermochemical software and databases, CALPHAD: Comput. Coupling Phase Diagrams Thermochem., 26 (2), 2002, pp. 189–228.

[9] Muller, J. and Steenkamp, J.D. An evaluation of thermochemical property models for CaO-MnO-SiO2-Al2O3-MgO. Ninth International Conference on Molten Slags, Fluxes and Salts (MOLTEN12), Beijing, China, 27–30 May 2012.

[10] Lienhard, J.H. IV and Lienhard, J.H. V. A Heat Transfer Textbook. 3rd edn. Phlogiston Press, Cambridge MA, 2006.

[11] MSDS:Morsil™ Nitride bonded silicon carbide, Thermal Ceramics Australia (Pty)Ltd., Beverley Park, South Australia.

[12] MSDS: SUPER DUTY High Grade Firebrick. Vereeniging Refractories (Pty) Ltd., Vereeniging, South Africa, 2005.

[13] McDougall, I., Smith, C.F.R., Olmstead, B., and Gericke, W.A. A finite element model of a Soderberg electrode with an application in casing design. Proceedings: Tenth International Ferroalloys Congress INFACON X: Transformation through Technology, Cape Town, South Africa, 1-4 February 2004, pp. 575-584.